


Article

Relationship between Textural Parameters of Lamellar Products Obtained by Acid Activation of Pure and Commercial Vermiculites and Their Iron and Water Content

Celia Marcos ^{1,*}, Alaa Adawy ²  and Irene Rodríguez ¹

¹ Geology Department & Organometallic Chemical Institute “Enrique Moles”, University of Oviedo, Jesús Arias de Velasco s/n, 33005 Oviedo, Asturias, Spain; ani@innova.uniovi.es

² Laboratory of High-Resolution Transmission Electron Microscopy, Institute for Scientific and Technological Resources, University of Oviedo, Edificio Severo Ochoa s/n, Campus de El Cristo, 33006 Oviedo, Asturias, Spain; hassanala@uniovi.es

* Correspondence: cmarcos@uniovi.es; Tel.: +34-985-10-3100

Received: 3 July 2020; Accepted: 22 July 2020; Published: 26 July 2020



Abstract: The relationship between textural parameters (specific superficial area (S_{BET}) and porosity (V_p)) of lamellar products obtained from HNO_3 -activated vermiculites and their iron and water content has been established. Two commercial vermiculites, one thermoexfoliated commercial vermiculite, and one pure vermiculite were nitric-acid-treated at 4 and 8 M concentrations for 1, 3, and 7 days. Untreated and treated samples were characterized with X-ray diffraction (XRD), scanning electron microscopy (SEM), high-resolution transmission electron microscopy (HRTEM), and N_2 physisorption analysis. The untreated vermiculites showed a direct relationship between their iron content and the values of S_{BET} , V_p , and pore size; an inverse relationship was observed in the case of the treated samples. The iron content may prevent further leaching of cations but not water loss, therefore forming lamellar products with lower S_{BET} and V_p values. The S_{BET} and V_p values of the studied thermoexfoliated sample were higher than those of the starting sample. The S_{BET} and V_p values of the activated thermoexfoliated sample were lower than those of the activated non-thermoexfoliated sample.

Keywords: vermiculite; thermoexfoliated vermiculite; nitric acid treatment; specific surface area; porosity

1. Introduction

Vermiculite in the strict sense is a layered silicate mineral with 2:1 crystalline structure composed of two T-O-T layers joined by an interlayer. The T-O-T layer is composed of an octahedral (O) sheet of Mg^{2+} , located between two tetrahedral sheets (T) of Si^{4+} . The interlayer is formed by an octahedral sheet of Mg^{2+} bound to oxygens or OH^- groups, and it contains water. Vermiculite shows a broad diversity in charged layers associated with numerous isomorphic substitutions, disorder effects, dehydration–rehydration ability, and swelling processes. The different hydration states were described by [1]. Commercial or industrial vermiculite consists of interstratified, diverse types of mica, mica-vermiculite [2], and interstratifications of vermiculite with different hydration states [3].

Vermiculites can be modified by changes in temperature and pressure, chemical treatments, and irradiation [3–14], causing physical and structural changes in the mineral that are very important for industrial and technological applications.

Acidic treatment is reported as a low-cost method to obtain materials possessing high porosity, a large number of acidic sites, and high specific surface area [15]. A large number of studies have been performed on the acidic activation of vermiculites using HCl and H₂SO₄ [15–25], and less studies have applied nitric acid as a leaching agent [15,24,26–30]. These studies have shown that the resulting products have high specific surface area and porosity [27,29] and are useful in various applications. They can be used as selective adsorbents for specific contaminants from wastewater [24,29–31], support for luminescent complexes [32], and selective catalysts for NO reduction [27].

In the present study, nitric acid treatment at 4 and 8 M was used at room temperature and for different treatment times on one pure vermiculite sample, two commercial vermiculites, and one thermoexfoliated commercial vermiculite. The objective was to establish the relationship between textural parameters, specific superficial area, and porosity of lamellar products obtained from those treated vermiculites and their iron and water content.

2. Materials and Methods

Vermiculites from Santa Olalla (Huelva, Spain), Goiás (Brazil), and China (provided by Vermiculita y Derivados S.A. company, Gijón, Spain), coded as V1, V2, and V3, respectively, were previously described and classified [3] as pure (V1) and commercial vermiculites (V2 and V3). The average diameter of the particles was: V1 ≤ 2 mm, V2 ≈ 1–2 mm and V3 ≈ 2 mm. The composition and water content [3] are in Table 1. The vermiculites were used as received, although other minerals (such as quartz and iron oxides) visible by the naked eye were removed before nitric acid treatment. In particular, V2 was dispersed in 400 mL of distilled water to remove iron oxides covering the particles. After several washes, V2 was filtered and dried at room temperature (25 °C).

Table 1. Chemical analyses (wt%) and water content of the starting vermiculites and thermoexfoliated vermiculites [3].

Oxides	V1	V2	V3	V2E	V3E
SiO ₂	35.93	40.67	35.65	40.60	36.34
Al ₂ O ₃	15.78	11.51	11.00	10.15	11.26
MgO	24.13	18.05	21.81	5.50	21.54
FeO	3.27	9.58	4.63	10.59	4.70
TiO ₂	0.33	0.79	1.16	1.30	1.35
Cr ₂ O ₃	0.03	0.01	0.39	0.04	0.32
K ₂ O	0.03	1.07	5.61	0.00	4.73
CaO	0.29	0.03	0.92	0.50	1.11
Na ₂ O	0.12	0.12	3.55	0.00	1.15
MnO	0.14	0.08	0.04	0.05	0.03
NiO	0.00	0.01	0.06	0.00	0.10
Water content	25.6	13.6	12.3	5.6	7.0

The nitric acid used in this study was of analytical grade (AnalaR NORMAPUR, 65% and $\rho = 1.45$ g/mL). The cleaned commercial vermiculites V2 and V3 were heated in an oven at 1000 °C, previously stabilized, for 1 min to exfoliate them. The vermiculite with the highest exfoliation coefficient was selected for subsequent nitric acid treatment.

One-gram samples of V1, V2, V3, and exfoliated V3 (V3E) were immersed in 25 mL of HNO₃ at two concentrations (4 and 8 mol/L) for 1, 3, and 7 days at room temperature. The solutions were periodically stirred manually. Afterwards, the samples were filtered and washed with distilled water multiple times to remove the acid. Finally, the resultant samples were dried at room temperature (25 °C).

Nitric acid treatment and physisorption experiments were continued with the exfoliated V3 sample because, as will be seen below, its exfoliation coefficient was the highest of the three samples.

The codes used for the samples treated in this study are given in the form VN-NM-ND, where the N associated with V is a number referring to the vermiculites V1, V2, and V3; the N associated with M is a number referring to the HNO₃ molarity used, either 4 or 8 M; and the N associated with D is a number referring to the days of treatment, either 1, 3, or 7.

One milliliter of each sample was weighed pre- and postacidic treatment, and the volume post-treatment was measured to quantify potential loss of mass or water and obtain the exfoliation coefficient ($k = \text{density of the raw sample} / \text{density of the treated sample}$ [33]) or determine the degree of delamination.

To identify any structural changes, X-ray diffraction patterns were recorded with a PANalytical X'pertPro diffractometer (Malvern Instruments, Malvern, UK) using 40 mA and 45 kV (Cu-K α radiation; $\lambda = 1.5418 \text{ \AA}$), 2θ scans 5° – 35° , 2θ step scans of 0.007° , and a counting time of 1 s per step. The standard reference material used was 660a NIST LaB6 with full width at half maximum (FWHM) of 0.06° for $2\theta = 21.36^\circ$. An aluminum sample holder was used for the powdered sample (0.5 g). For the phase identification, the PANalytical software (Version 4.8, X'Pert Plus, Worcestershire, UK) was used.

Elemental analyses of untreated and treated samples were obtained using a JEOL 6610LV scanning electron microscope (JEOL, Tokyo, Japan) with a scattered X-ray energy microanalyzer EDX (INCA Energy 2000, Oxford Instruments, Abingdon, UK) with an acceleration voltage of 20 kV with probe current intensity fitting for 25% void time on spectrum calibration with Cu. Samples were glued to an aluminum support with a double-sided carbon adhesive and coated with a gold layer (100 Å thickness) to make it conductive. To obtain the highest precision and best statistics of the results, the analyses were carried out by zones no smaller than 0.1 mm^2 on very flat surfaces.

A 200 keV field emission gun, JEOL JEM-2100F TEM high-resolution microscope with a resolution of 1.9 Å between points and 1.0 Å between lines was used to obtain TEM and selected area electron diffraction (SAED) micrographs with its accompanying CCD camera (Gatan). The associated microanalyzer EDX (X-max, Oxford instruments) was used together with bright field detector (EM24541SIOD, JEOL) in STEM mode to obtain elemental mapping of several projections of the samples, for which INCA software was used.

Textural parameters of the powdered samples were determined with the ASAP 2020 equipment under the following conditions: nitrogen adsorption at -195.8 K , with $\sigma_m (\text{N}_2)$ of 0.162 nm^2 ; unrestricted evacuation of 30.0 mm Hg; vacuum pressure of 10 $\mu\text{m Hg}$; evacuation time of 1 h; and temperature of sample evacuation prior to N₂ adsorption measurements of 22°C . The data were recorded with equilibration times (p/p_0 between 0.001 and 1.000) between 50 and 25 s and a minimum equilibrium delay of 600 s at $p/p_0 \geq 0.995$. Specific surface area and pore size data have been determined by using a mathematical description of the adsorption isotherms with the software of the equipment.

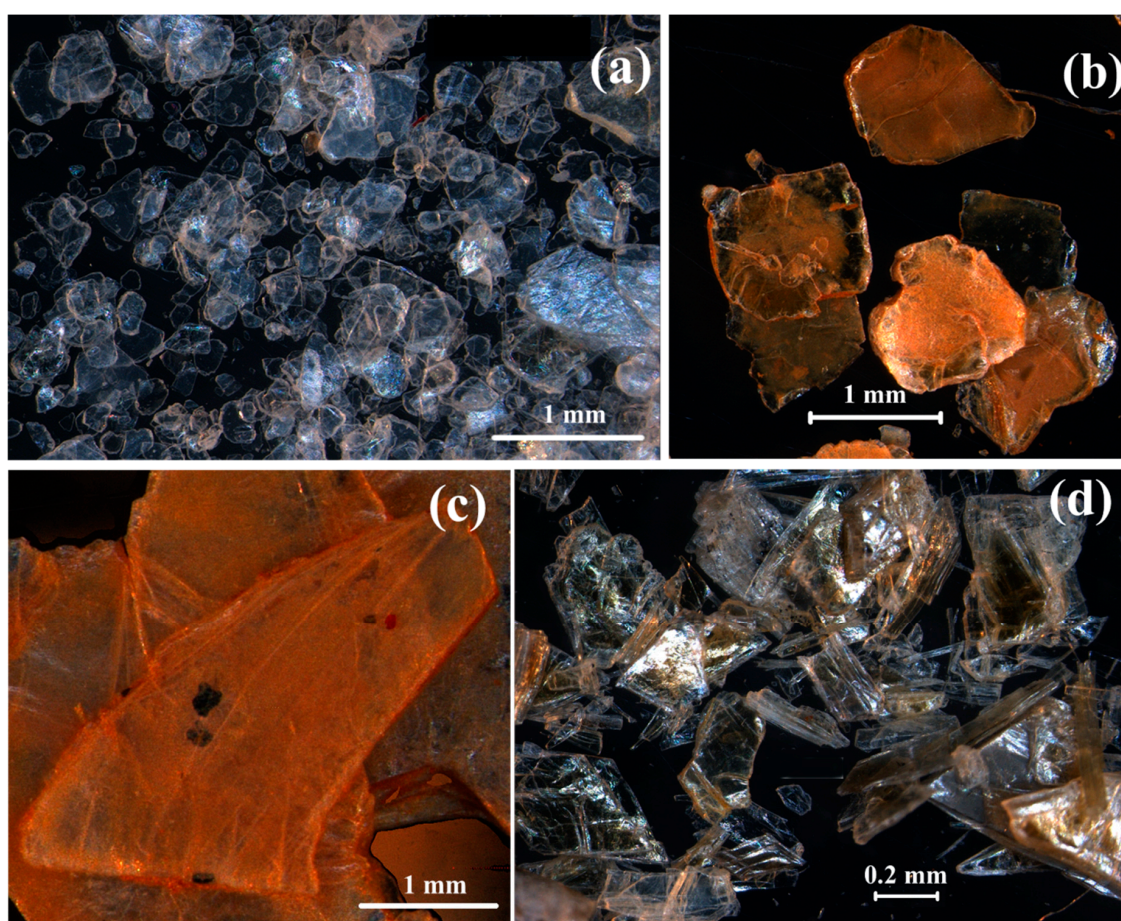
Photos of post-treatment samples were taken with a Leica stereo microscope coupled with Leica IC 3D camera.

3. Results

Vermiculites treated with acid suffered a slight delamination. These vermiculites also suffered a loss of color and weight (Table 2), which is due to the loss of mass and water. Samples V1-4M-1D, V1-4M-7D, V1-8M-1D, and V1-8M-7D (with low cation, e.g., iron, concentrations) were practically colorless (Figure 1a). This was also the case for V3-4M-7D and V3-8M-7D. Sample V2-4M-1D maintained its coppery color, and its particle size decreased. Sample V2-4M-7D possessed a lighter color (Figure 1b) and showed rounded iron oxide particles adhered between the layers of vermiculite (Figure 1c). V3-4M-1D and V3-8M-1D turned to golden-green, became more transparent, and showed a reduction in particle size.

Table 2. Weight loss (%) in the treated samples.

Samples	Weight Loss (%)
V1-4M-1D	70
V1-8M-1D	75
V1-4M-7D	72
V1-8M-7D	70
V2-4M-1D	12
V2-8M-1D	14
V2-4M-7D	47
V2-8M-7D	47
V3-4M-1D	22
V3-8M-1D	27
V3-4M-7D	53
V3-8M-7D	52

**Figure 1.** Micrographs of treated vermiculites: (a) V1-4M-7D; (b) V2-4M-7D; (c) iron oxide particles in V2-4M-7D; (d) V3-4M-7D.

The exfoliation coefficients for V2 and V3 after heating treatment were 7.4 and 6.1, respectively. These values are much higher than those of V1. The exfoliation coefficients for V1 were between 1.70 and 2.09 and are considered very pure [33].

Figure 2 shows the XRD patterns of V1, V2, V3, V3E pre- and post lixiviation for 7 days with 4 and 8 M HNO₃, along with the percentages of the phases present in each treated sample. Vermiculites treated with acid suffered structural transformation that resulted in the formation of lamellar products with low crystallinity and order.

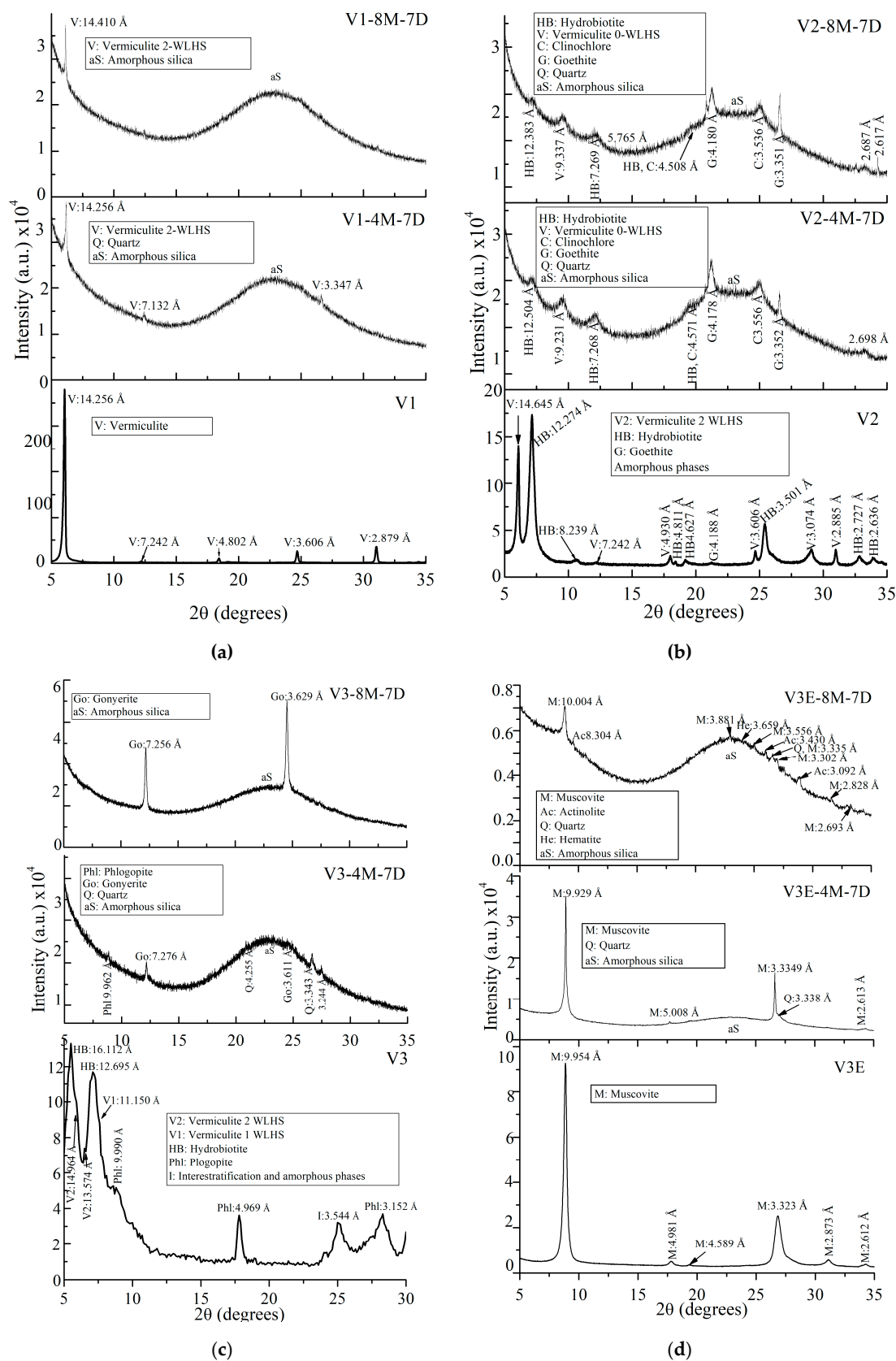


Figure 2. X-ray diffraction patterns of V1 (a), V2 (b), V3 (c), and V3E (d) pre- and post treatment.

The XRD analysis confirmed the purity of V1, composed of vermiculite with two water layers in the interlayer (2-WLHS) (JCPDS card 16-613). V2 consisted of vermiculite 2-WLHS (JCPDS card 16-613); hydrobiotite (JCPDS card 13-465); two interstratified phases (one of them at 8.24 Å, attributed to a biotite/vermiculite layer with regular interstratifications [34], and the other at 3.5 Å, attributed to a mixed-layer phase of vermiculite/chlorite); and goethite (JCPDS card 29-713) in a very low proportion. In the V3 sample, hydrobiotite and vermiculite 2-WLHS and 1-WLHS coexisted with a mixed-layer phase of vermiculite/chlorite at 3.5 Å and phlogopite (JCPDS 16-334).

The lamellar products consisted of amorphous silica and other phases shown in Figure 2, which varied depending on the vermiculite type. Therefore, XRD patterns reflected the loss of the leaching cations, which occurred according to the following order: V1 > V3 > V2.

The elemental analyses provided by EDX combined with scanning electron microscopy of the untreated and treated samples are shown in Table 3.

Table 3. Elemental analyses (at %) for V1, V2, and V3 pre- and post-treatment with 4 and 8 M nitric acid for 7 days.

Sample	O	Si	Mg	Al	Fe	Ti	Cr	Ca	Na	K
V1	69.4 (2.8)	11.4 (1.1)	12.1 (0.4)	5.7 (0.3)	1.3 (0.9)	0.1 (0.0)		0.1 (0.1)		
V1-4M-7D	73.7 (0.6)	26.3 (0.6)								
V1-8M-7D	70.0 (2.8)	30.0 (2.8)								
V2	67.6 (1.5)	12.7 (0.8)	9.8 (1.0)	4.4 (0.3)	2.8 (0.8)	0.8 (0.1)				2.3 (0.4)
V2-4M-7D	67.8 (1.8)	28.8 (3.9)		2.1 (2.3)	1.0 (0.3)	0.4 (0.2)				
V2-8M-7D	66.6 (3.3)	31.2 (3.5)		0.5 (0.6)	1.1 (0.2)	0.5 (0.1)				
V3	66.2 (1.6)	13.0 (0.7)	11.8 (0.3)	4.5 (0.2)	1.2 (0.2)	0.3 (0.1)	0.1 (0.0)	0.4 (0.1)	1.0 (0.2)	1.7 (0.3)
V3-4M-7D	75.1 (4.4)	24.7 (4.7)								
V3-8M-7D	77.0 (2.5)	19.9 (5.5)								

HRTEM was useful for monitoring particles after the nitric acid treatment, such as hematite in V1-8M-7D (Figure 3) or hematite and goethite with atomic composition of 27.85% Fe, 63.07% O, 4.35% Al, 1.69% Si, 2.82% Ti, and 0.21% Cr in V2-4M-7D (Figure 4a–f).

The nitrogen adsorption–desorption isotherms of the untreated vermiculites and the vermiculites treated with nitric acid are shown in Figure 5. The isotherms of the treated vermiculites could be of type IV, showing characteristics of mesoporous solids [35]. The slight hysteresis H3 shown by V2 and V3 samples is a characteristic of plate-like particles of vermiculites [35].

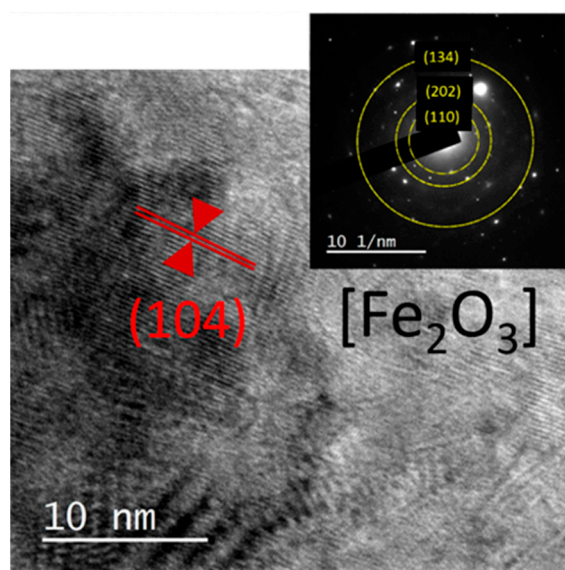


Figure 3. Micrographs of V1-8M-7D with HRTEM showing lattice fringes corresponding to hematite, with the corresponding selected area electron diffraction (SAED) pattern in the inset micrograph.

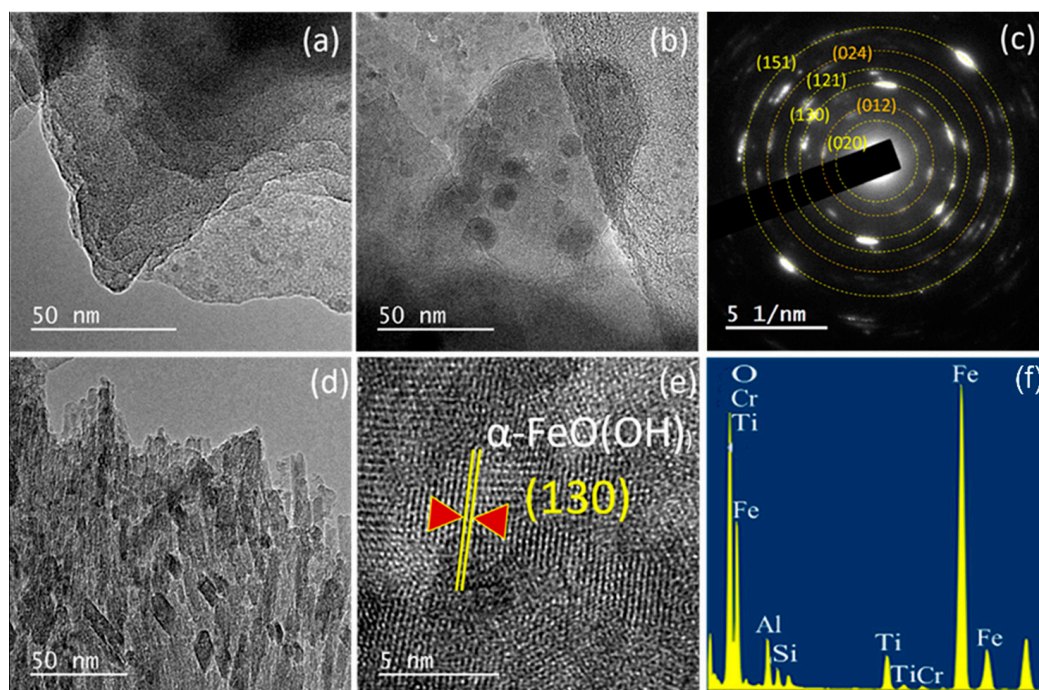


Figure 4. HRTEM micrographs of V2-4M-7D: (a) well-layered structures; (b) small, rounded iron particles; (c) SAED of polycrystalline goethite shown in (d); (e) magnified view of (d) showing d_{hkl} corresponding to goethite (α -FeO(OH)); (f) the spectrum of V2-4M-7D.

The specific surface area (S_{BET}), adsorption capacity (Q_m), total pore volume (V_p), pore size (nm), BET constant (C), and correlation coefficient (R^2) values obtained from the adsorption–desorption tests are shown in Table 4. The BET constant (C) values of the investigated untreated and treated samples confirmed that microspores are not present, indicating the validity of the BET method.

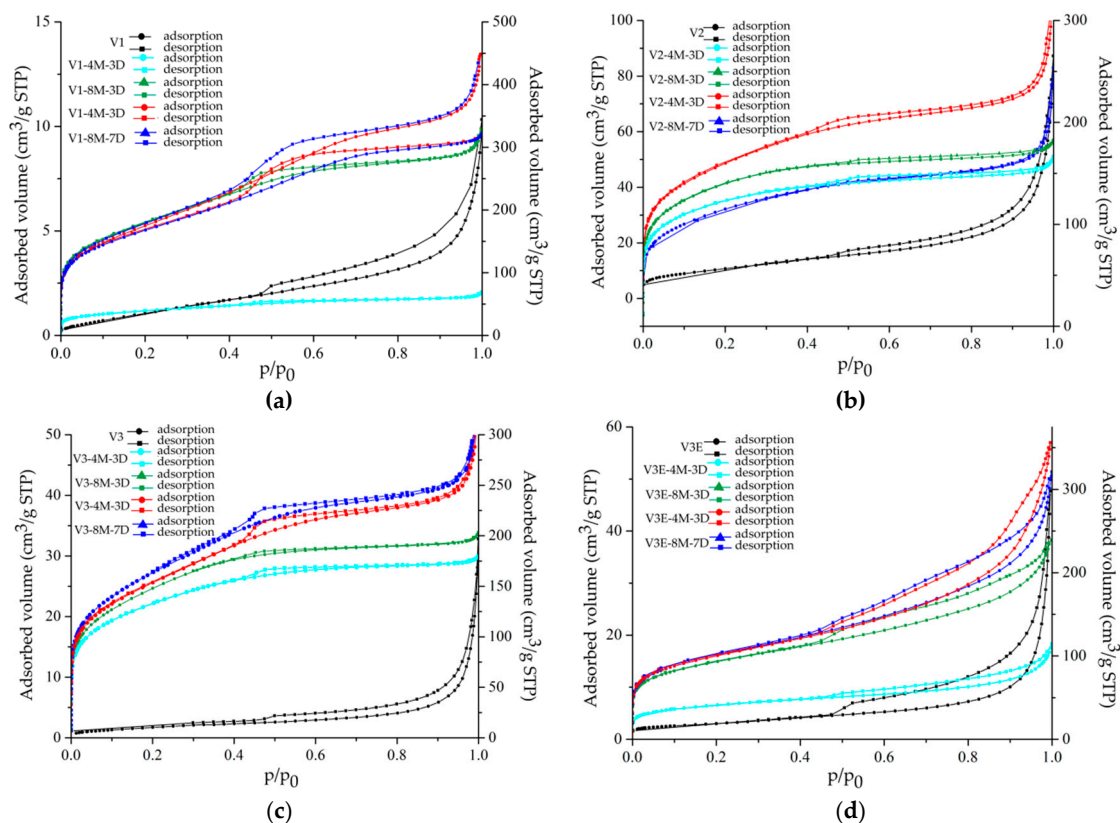


Figure 5. Nitrogen adsorption–desorption isotherms of V1 (a), V2 (b), V3 (c), and V3E (d). Note: The right ordinate scale is for the untreated samples; the left ordinate scale is for the treated samples.

Table 4. Specific surface area (S_{BET}), adsorption capacity (Q_m), pore volume (V_p), BET constant (C), and correlation coefficient (R^2) results from adsorption–desorption nitrogen measurements for V1, V2, V3, and their treated counterparts.

Sample	S_{BET} (m^2/g)	Q_m ($\text{cm}^3/\text{g STP}$)	V_p ($\text{cm}^3/\text{g STP}$)	Pore Size (nm)	C	R^2
V1	3 ± 0	0.7	0.01	2.38	61	0.99528
V1-4M-3D	138 ± 0	32	0.09	1.69	194	0.99992
V1-8M-3D	598 ± 6	137	0.54	1.69	286	0.99942
V1-4M-7D	537 ± 6	123	0.48	1.72	401	0.99950
V1-8M-7D	586 ± 4	135	0.56	2.53	218	0.99970
V2	36 ± 0	9	0.09	2.65	136	0.99963
V2-4M-3D	411 ± 4	94	0.08	2.56	525	0.99952
V2-8M-3D	465 ± 4	107	0.08	2.57	437	0.99971
V2-4M-7D	513 ± 9	118	0.27	2.52	712	0.99869
V2-8M-7D	389 ± 4	89	0.28	1.80	324	0.99972
V3	7 ± 0	1.6	0.03	2.52	28	0.99965
V3-4M-3D	419 ± 6	96	0.09	2.58	592	0.99949
V3-8M-3D	505 ± 4	116	0.13	2.54	237	0.99971
V3-4M-7D	510 ± 6	117	0.27	2.79	361	0.99924
V3-8M-7D	510 ± 6	117	0.33	2.48	602	0.99891
V3E	11 ± 0	2.5	0.07	3.08	135	0.99998
V3E-4M-3D	148 ± 0	34	0.07	3.09	213	0.99998
V3E-8M-3D	284 ± 0	65	0.29	3.08	165	0.99999
V3E-4M-7D	358 ± 1	82	0.44	3.11	222	0.99997
V3E-8M-7D	331 ± 1	77	0.26	3.08	222	0.99999

The S_{BET} , V_p , and pore size values of the starting samples follow the relationship $V2 > V3 > V1$, and this same relationship is observed for the iron content. Meanwhile, S_{BET} and V_p values of the nitric-acid-treated samples follow the inverse relationship, with the pore size values of treated samples being more variable. The S_{BET} and V_p values of the V3E sample were higher than those of the V3 sample, but the S_{BET} values of the treated samples were lower than the S_{BET} value of the starting sample. In terms of porosity, some of the treated thermoexfoliated samples, such as V3E-4M-7D, reached a higher value than that of the treated samples without exfoliation. Regarding the pore size, there was no difference between the untreated thermoexfoliated sample and the treated exfoliated ones, and their values were the highest of the samples investigated.

4. Discussion

The loss of crystallinity and order experienced by the treated vermiculites is probably due not only to the loss of mass but also to the loss of structural water, as observed with other treatments such as temperature increase [10], vacuum [36], microwave irradiation [11], and alcohol [37,38].

Hematite and goethite were detected and analyzed with HRTEM in V1-8M-7D but were not detectable with XRD, probably due to their lower proportion and nanometric size. The partial leaching of cations from the octahedral sheets of the studied vermiculites as a result of the acidic treatment probably occurred so that iron could be transferred from those octahedral sheets to clusters deposited on vermiculite layers [17,25,39,40].

The high porosity and specific surface area of the lamellar products obtained from the nitric-acid-treated V1 samples are due to the fact that these samples suffered greater leaching of cations and water loss than the nitric-acid-treated V2 and V3 samples, whose high iron content may have prevented further leaching of other cations, producing less porosity and specific surface area. This fact also explains the difference in weight loss between the investigated vermiculites. In addition, said treatment depends on the particle size. As seen in other chemical and thermal treatments, a larger particle size is responsible for a slower dissolution [3,11,14]. In any case, the resulting products of the vermiculites treated with nitric acid, namely silica and other phases that varied depending on vermiculite type, were formed as a consequence of the structural water loss, in addition to the loss of cations due to leaching.

The decrease of the S_{BET} values at a higher acid concentration in the V2 vermiculite was also observed in other vermiculites [18,29,41,42]; this could be because it reached its maximum leaching with 4 M HNO_3 and then decreased with the increase in acid concentration, although the porosity did not decrease. The S_{BET} value of the V3E sample was higher than that of the V3 sample, probably due to lower water content in the former. The nitric-acid-treated V3E samples, composed of mica muscovite, exhibited higher resistance to dissolution than the activated non-thermoexfoliated sample in which several phases coexisted [19,43]. Thermoexfoliated vermiculites like the sample from China can be very suitable for removing heavy metals from aqueous solutions because its S_{BET} is twice that of its counterpart that was not thermoexfoliated. The opposite occurred for the activated thermoexfoliated sample, as it exhibited lower resistance to dissolution than the activated non-thermoexfoliated sample.

The differences in the S_{BET} and V_p values of the untreated and treated vermiculites are due to the differences in the iron content of the starting vermiculites. The higher the iron content of the initial sample, the higher the S_{BET} , V_p , and pore size values of the starting sample. In the acid-activated samples, the opposite relationship is observed. In the samples with high iron content, this element may have prevented further leaching of cations but not water loss, therefore granting the lamellar products formed with lower specific surface area and porosity. These relationships could be very important when selecting vermiculite to obtain a product with a high specific surface area and porosity after acidic treatment.

Author Contributions: Conceptualization, C.M.; methodology, C.M., A.A., and I.R.; investigation, C.M., A.A., and I.R.; resources, C.M., A.A., and I.R.; writing—original draft preparation, C.M.; writing—review and editing, C.M. and A.A.; project administration, C.M. and A.A.; funding acquisition, C.M. and A.A. All authors have read and agreed to the published version of the manuscript.

Funding: This research was funded by Oviedo University (Spain), grant number PAPI18-EMERG-13; by Spanish MINECO, grant number MAT2016-78155-C2-1-R; and by the Government of the Principality of Asturias, grant number GRUPIN-IDI/2018/170.

Acknowledgments: The authors wish to acknowledge the Scientific-Technical Services of Oviedo University (Spain) for obtaining the X-ray patterns and SEM and TEM analysis, as well as the reviewers and editor for the manuscript revision.

Conflicts of Interest: The authors declare no conflict of interest.

References

1. Suzuki, M.; Wada, N.; Hines, D.R.; Whittingham, M.S. Hydration states and phase transitions in vermiculite intercalation compounds. *Phys. Rev. B* **1987**, *36*, 2844–2851. [\[CrossRef\]](#)
2. Walker, G.F. Trioctahedral minerals in the soil clays of North East Scotland. *Mineral. Mag. J. Mineral. Soc.* **1951**, *29*, 72–84. [\[CrossRef\]](#)
3. Marcos, C.; Arango, Y.C.; Rodríguez, I. X-ray diffraction studies of the thermal behaviour of commercial vermiculites. *Appl. Clay Sci.* **2009**, *42*, 368–378. [\[CrossRef\]](#)
4. Myers, J.B. Vermiculite. In *Industrial and Minerals Rocks*; American Institute of Mechanical Engineers: New York, NY, USA, 1963; pp. 889–895.
5. Mamina, A.K.; Kotelnikova, E.N.; Muromtsev, V.A. Influence of the structural perfection of phlogopite crystals on their cleavability by hydrogen peroxide. *Inorg. Mater.* **1990**, *26*, 2104–2107.
6. Suquet, H.; Chevalier, S.; Marcilly, C.; Barthomeuf, D. Preparation of porous materials by chemical activation of the Llano vermiculite. *Clay Miner.* **1991**, *26*, 49–60. [\[CrossRef\]](#)
7. Üçgül, E.; Girgin, I.Ç. Chemical exfoliation characteristics of Karakoc, phlogopite in hydrogen peroxide solution. *Turk. J. Chem.* **2002**, *26*, 431–439.
8. Obut, A.; Girgin, I.Ç. Hydrogen peroxide exfoliation of vermiculite and phlogopite. *Miner. Eng.* **2002**, *15*, 683–687. [\[CrossRef\]](#)
9. Weiss, Z.; Valášková, M.; Seidlerová, J.; Šupová-Křístková, M.; Šustai, O.; Matějka, V. Preparation of vermiculite nanoparticles using thermal hydrogen peroxide treatment. *J. Nano Sci. Nano Technol.* **2006**, *6*, 726–730. [\[CrossRef\]](#)
10. Marcos, C.; Rodríguez, I. Expansion behaviour of commercial vermiculites at 1000 °C. *Appl. Clay Sci.* **2010**, *48*, 492–498. [\[CrossRef\]](#)
11. Marcos, C.; Rodríguez, I. Expansibility of vermiculites irradiated with microwaves. *Appl. Clay Sci.* **2011**, *51*, 33–37. [\[CrossRef\]](#)
12. Marcos, C.; Rodríguez, I. Exfoliation of vermiculites with chemical treatment using hydrogen peroxide and thermal treatment using microwaves. *Appl. Clay Sci.* **2014**, *87*, 219–227. [\[CrossRef\]](#)
13. Huo, X.; Wu, L.; Liao, L.; Xia, Z.; Wang, L. The effect of interlayer cations on the expansion of vermiculite. *Powder Technol.* **2012**, *224*, 241–246. [\[CrossRef\]](#)
14. Hillier, S.; Marwa, E.M.M.; Rice, C.M. On the mechanism of exfoliation of Vermiculite. *Clay Miner.* **2013**, *48*, 563–582. [\[CrossRef\]](#)
15. Jin, L.; Dai, B. TiO₂ activation using acid-treated vermiculite as a support: Characteristics and photoreactivity. *Appl. Surf. Sci.* **2012**, *258*, 3386–3392. [\[CrossRef\]](#)
16. Suquet, H.; Franck, R.; Lambert, J.E.; Marcilly, C.E.E.; Chevalier, S. Catalytic properties of two pre-cracking matrices; a leached vermiculite and a Al-pillared saponite. *Appl. Clay Sci.* **1994**, *8*, 349–364. [\[CrossRef\]](#)
17. Ravichandran, J.; Sivasankar, B. Properties and catalytic activity of acid-modified montmorillonite and vermiculite. *Clays Clay Miner.* **1997**, *45*, 854–858. [\[CrossRef\]](#)
18. Temuujin, J.; Okada, K.; MacKenzie, K.J.D. Preparation of porous silica from vermiculite by selective leaching. *Appl. Clay Sci.* **2003**, *22*, 187–195. [\[CrossRef\]](#)
19. Okada, K.; Arimitsu, N.; Kameshima, Y.; Nakajima, A.; MacKenzie, K.J.D. Solid acidity of 2:1 type clay minerals activated by selective leaching. *Appl. Clay Sci.* **2006**, *31*, 185–196. [\[CrossRef\]](#)

20. Maqueda, C.; Romero, A.S.; Morillo, E.; Perez-Rodriguez, J.L. Effect of grinding on the preparation of porous materials by acid-leached vermiculite. *J. Phys. Chem. Solids* **2007**, *68*, 1220–1224. [[CrossRef](#)]
21. Maqueda, C.; Perez-Rodriguez, J.L.; Šubrt, J.; Murafa, N. Study of ground and unground leached vermiculite. *Appl. Clay Sci.* **2009**, *44*, 178–184. [[CrossRef](#)]
22. Perez-Rodriguez, J.L.; Maqueda, C.; Murafa, N.; Šubrt, J.; Balek, V.; Pulišová, P.; Lančok, A. Study of ground and unground leached vermiculite II. Thermal behaviour of ground acid-treated vermiculite. *Appl. Clay Sci.* **2011**, *51*, 274–282. [[CrossRef](#)]
23. Steudel, A.; Batenburg, L.F.; Fischer, H.R.; Weidler, P.G.; Emmerich, K. Alteration of swelling clay minerals by acid activation. *Appl. Clay Sci.* **2009**, *44*, 105–115. [[CrossRef](#)]
24. Stawiński, W.; Freitas, O.; Chmielarz, L.; Węgrzyn, A.; Komędera, K.; Mordarski, G.; Figueiredo, S. The influence of acid treatments over vermiculite based material as adsorbent for cationic textile dyestuffs. *Chemosphere* **2016**, *153*, 115–129. [[CrossRef](#)] [[PubMed](#)]
25. Komadel, P. Acid activated clays: Materials in continuous demand. *Appl. Clay Sci.* **2016**, *131*, 84–99. [[CrossRef](#)]
26. Del Rey-Perez-Caballero, F.J.; Poncelet, G. Microporous 18 angstrom Al-pillared vermiculites: Preparation and characterization. *Microporous Mesoporous Mater.* **2000**, *41*, 169–181. [[CrossRef](#)]
27. Chmielarz, L.; Kowalczyk, A.; Michalik, M.; Dudek, B.; Piwowarska, Z.; Matusiewicz, A. Acid-activated vermiculites and phlogophites as catalysts for the DeNOx process. *Appl. Clay Sci.* **2010**, *49*, 156–162. [[CrossRef](#)]
28. Alves, A.P.M.; Fonseca, M.G.; Wanderley, A.F. Inorganic-organic Hybrids Originating from Organosilane Anchored onto Leached Vermiculite. *Mater. Res.* **2013**, *16*, 891–897. [[CrossRef](#)]
29. Santos, S.S.G.; Silva, H.R.M.; de Souza, A.G.; Alves, A.P.M.; da Silva Filho, E.C.; Fonseca, M.G. Acid-leached mixed vermiculites obtained by treatment with nitric acid. *Appl. Clay Sci.* **2015**, *104*, 286–294. [[CrossRef](#)]
30. Węgrzyn, A.; Stawiński, W.; Freitas, O.; Komędera, K.; Błachowski, A.; Jęczmionek, Ł.; Dańko, T.; Mordarski, G.; Figueiredo, S. Study of adsorptive materials obtained by wet fine milling and acid activation of vermiculite. *Appl. Clay Sci.* **2018**, *155*, 37–49. [[CrossRef](#)]
31. Polubesova, T.; Zadaka, D.; Groisman, L.; Nir, S. Water remediation by micelleclay system: Case study for tetracycline and sulfonamide antibiotics. *Water Res.* **2006**, *40*, 2369–2374. [[CrossRef](#)]
32. Silva, H.R.M.; Fonseca, M.G.; Espinola, J.G.P.; Brito, H.F.; Fasustino, W.M.; Teotonio, E.E.S. Luminescent Eu-III complexes immobilized on a vermiculite clay surface. *Eur. J. Inorg. Chem.* **2014**, *11*, 1914–1921. [[CrossRef](#)]
33. Justo, A.; Maqueda, C.; Pérez Rodriguez, J.L.; Morillo, E. Expansibility of some vermiculites. *Appl. Clay Sci.* **1989**, *4*, 509–519. [[CrossRef](#)]
34. Harraz, H.Z.; Hamdy, M.M. Interstratified vermiculite–mica in the gneiss–metapelite–serpentine rocks at Hafafit area, Southern Eastern Desert, Egypt: From metasomatism to weathering. *J. Afr. Earth Sci.* **2010**, *58*, 305–320. [[CrossRef](#)]
35. Thommes, M.; Kaneko, K.; Neimark, A.V.; Olivier, J.P.; Rodriguez-Reinoso, F.; Rouquerol, J.; Sing, K.S.W. Physisorption of gases, with special reference to the evaluation of surface area and pore size distribution (IUPAC Technical Report). *Pure Appl. Chem.* **2015**, *87*, 1051–1069. [[CrossRef](#)]
36. Marcos, C.; Argüelles, A.; Ruiz-Conde, A.; Sánchez-Soto, P.J.; Blanco, J.A. Study of the dehydration process of vermiculites by applying a vacuum pressure: Formation of interstratified phases. *Mineral Mag.* **2003**, *67*, 1253–1268. [[CrossRef](#)]
37. Marcos, C.; Rodriguez, I. Structural changes on vermiculite treated with methanol and ethanol and subsequent microwave irradiation. *Appl. Clay Sci.* **2016**, *123*, 304–314. [[CrossRef](#)]
38. Marcos, C. and Rodriguez, I. Effect of propanol and butanol and subsequent microwave irradiation on the structure of commercial vermiculites. *Appl. Clay Sci.* **2017**, *144*, 104–114. [[CrossRef](#)]
39. Wypych, F.; Adad, L.B.; Mattoso, N.; Marangon, A.A.S.; Schreiner, W.H. Synthesis and characterization of disordered layered silica obtained by selective leaching of octahedral sheets from chrysotile and phlogopite structures. *J. Colloid Interface Sci.* **2005**, *283*, 107–112. [[CrossRef](#)]
40. Chmielarz, L.; Wojciechowska, M.; Rutkowska, M.; Adamski, A.; Węgrzyn, A.; Kowalczyk, A.; Dudek, B.; Boron, P.; Michalik, M.; Matusiewicz, A. Acid activated vermiculites as catalysts of the DeNOx process. *Catal. Today* **2012**, *191*, 25–31. [[CrossRef](#)]

41. Yu, X.; Wei, C.; Ke, L.; Wu, H.; Chai, X.; Hu, Y. Preparation of trimethylchlorosilanemodified acid vermiculites for removing diethyl phthalate from water. *J. Colloid Interface Sci.* **2012**, *369*, 344–351. [[CrossRef](#)]
42. Ehsani, I.; Turianicová, E.; Baláž, M.; Obut, A. Effects of sulphuric acid dissolution on the physical and chemical properties of a natural and a heated vermiculite. *Acta Montanistica Slovaca* **2015**, *20*, 110–115.
43. Harkonen, M.A.; Keiski, R.A. Porosity and surface area of acid leached phlogopite. The effect of leaching conditions and thermal treatment. *Colloids Surf.* **1984**, *11*, 323–339. [[CrossRef](#)]



© 2020 by the authors. Licensee MDPI, Basel, Switzerland. This article is an open access article distributed under the terms and conditions of the Creative Commons Attribution (CC BY) license (<http://creativecommons.org/licenses/by/4.0/>).